

# Effects of the entrance channel mass asymmetry in fusion reactions<sup>\*</sup>

BIAN Bao-An(卞宝安)<sup>1;1)</sup> ZHANG Feng-Shou(张丰收)<sup>2,3</sup>

<sup>1</sup> School of Science, Jiangnan University, Wuxi 214122, China

<sup>2</sup> The Key Laboratory of Beam Technology and Material Modification of Ministry of Education, College of Nuclear Science and Technology, Beijing Normal University, Beijing 100875, China

<sup>3</sup> Center of Theoretical Nuclear Physics, National Laboratory of Heavy Ion Accelerator of Lanzhou, Lanzhou 730000, China

**Abstract** The symmetric and asymmetric fusion reaction systems forming the same compound nuclei  $^{26}\text{Al}$ ,  $^{30}\text{Si}$ ,  $^{38}\text{Ar}$  and  $^{170}\text{Hf}$  are investigated with the frame of improved isospin dependent quantum molecular dynamics model. The entrance channel mass asymmetry dependence of compound nucleus formation is found by analyzing the shell correction energies, the Coulomb barriers and the fusion cross sections. The calculated fusion cross sections agree quantitatively with the experimental data. The results indicate that compound nucleus formation is favorable for the systems with larger mass asymmetry because of the smaller Coulomb contribution to the fusion barrier.

**Key words** fusion reactions, mass asymmetry, Coulomb barrier

**PACS** 25.70.-z, 25.60.Pj, 24.10.-i

## 1 Introduction

In recent years, with the increasing availability of radioactive ion beams, heavy-ion fusion reactions at energies below and near the Coulomb barrier have attracted considerable attention. One can investigate the properties of nuclei far from the  $\beta$  stability by radioactive nuclear beam, especially for the synthesis of superheavy elements (SHEs). Different models have predicted the different superheavy “island of stability” around 114, 120, 124 or 126 protons and 184 neutrons [1–5]. Therefore, many experiments are carried out to find the superheavy “island of stability”, such as the elements 107 to 112 synthesized in cold fusion reactions [6, 7], and the elements from 113 to 116 and 118 produced in hot fusion reactions [8]. Many methods have been established to understand the fusion mechanism of SHE formation [9–11]. Experimental data can be reproduced and some new results have been predicted with these models. The models differ from each other, sometimes using contradictory

physical ideas. A microscopic description of the synthesis mechanism of SHEs remains a challenge to the microscopic theory.

Because of the extremely small cross section, the production of superheavy nuclei is difficult experimentally. In order to successfully synthesize the superheavy nucleus, it is very important to select the optimal combination of target and projectile, and the favorable bombarding energy. The study of the role of the entrance channel mass asymmetry ( $|A_2 - A_1| / (A_1 + A_2)$ ) in the fusion reaction is a relevant problem in establishing the optimal conditions for the synthesis of SHEs. The entrance channel mass asymmetry dependence of compound nucleus formation has been studied by the statistical model [12, 13] and the dinuclear systems model [14] for the asymmetric and nearly symmetric systems. In previous work, we concluded that compound nucleus formation is favorable for the system with a larger mass asymmetry [16]. Attempts to systematically understand the effects of an entrance channel for the systems with different mass

Received 14 November 2009

<sup>\*</sup> Supported by National Natural Science Foundation of China (10847136), Fundamental Research Funds for the Central Universities (JUSRP10911), National Program on Key Basic Research Project (G2010CB832903) and Specialized Research Fund for the Doctoral Programme of Higher Education of China (200800270017)

1) E-mail: baoanbian@163.com

©2010 Chinese Physical Society and the Institute of High Energy Physics of the Chinese Academy of Sciences and the Institute of Modern Physics of the Chinese Academy of Sciences and IOP Publishing Ltd

asymmetries are expected. In this work, we will investigate the entrance channel mass asymmetry dependence of compound nucleus formation for the fusion reactions  $^{12}\text{C}+^{14}\text{N}$ ,  $^{10}\text{B}+^{16}\text{O}$ ,  $^{17}\text{O}+^{13}\text{C}$ ,  $^{18}\text{O}+^{12}\text{C}$ ,  $^{19}\text{F}+^{19}\text{F}$ ,  $^{11}\text{B}+^{27}\text{Al}$ ,  $^{32}\text{S}+^{138}\text{Ba}$  and  $^{28}\text{Si}+^{142}\text{Ce}$  using the improved isospin dependent quantum molecular dynamics (ImIQMD) model [15–17].

## 2 Model and method

In the ImIQMD model, each nucleon is represented by a coherent state of a Gaussian wave packet,

$$\phi_i(\mathbf{r}, t) = \frac{1}{(2\pi\sigma_r)^{3/4}} \exp\left[-\frac{(\mathbf{r}-\mathbf{r}_i(t))^2}{4\sigma_r^2} + \frac{i\mathbf{p}_i(t)\cdot\mathbf{r}}{\hbar}\right], \quad (1)$$

where  $\mathbf{r}_i(t)$  and  $\mathbf{p}_i(t)$  are the centers of the  $i$ th wave packet in the coordinate and momentum space, respectively.  $\sigma_r$  is the width of the wave packet in the coordinate space [18]. It is well known that the nucleons are localized for a finite system in a finite region corresponding to the size of the system. Thus we consider a system size dependent wave packet width here. That is,

$$\sigma_r = 0.09A^{1/3} + 0.88. \quad (2)$$

Here,  $A$  is the number of nucleons bound in the system.

Through a Wigner transformation of the wave function, the  $N$ -body phase space distribution function is given by

$$f(\mathbf{r}, \mathbf{p}, t) = \sum_i f_i(\mathbf{r}, \mathbf{p}, t), \quad (3)$$

$$f_i(\mathbf{r}, \mathbf{p}, t) = \frac{1}{(\pi\hbar)^3} \exp\left[-\frac{(\mathbf{r}-\mathbf{r}_i(t))^2}{2\sigma_r^2} - \frac{(\mathbf{p}-\mathbf{p}_i(t))^2 \cdot 2\sigma_r^2}{\hbar^2}\right]. \quad (4)$$

The density distribution in the coordinate and momentum space are represented by

$$\begin{aligned} \rho(\mathbf{r}, t) &= \int f(\mathbf{r}, \mathbf{p}, t) d^3p \\ &= \sum_i \frac{1}{(2\pi\sigma_r^2)^{3/2}} \exp\left[-\frac{(\mathbf{r}-\mathbf{r}_i)^2}{2\sigma_r^2}\right], \end{aligned} \quad (5)$$

$$\begin{aligned} g(\mathbf{p}, t) &= \int f(\mathbf{r}, \mathbf{p}, t) d^3r \\ &= \sum_i \frac{1}{(2\pi\sigma_p^2)^{3/2}} \exp\left[-\frac{(\mathbf{p}-\mathbf{p}_i)^2 \cdot 2\sigma_p^2}{\hbar^2}\right], \end{aligned} \quad (6)$$

where  $\sigma_p$  is the width of the wave packet in momentum space.  $\sigma_r$  and  $\sigma_p$  satisfy the minimum uncertainty relation.

In order to describe the nucleon's Fermionic nature, an approximative treatment of an antisymmetrization, phase space constrain method is adopted [19]. It is required by the constraint that the occupation number in a volume  $h^3$  of the one body phase space around the point of  $(\mathbf{r}_i(t), \mathbf{p}_i(t))$ , which is the centroid of the  $i$ th wave packet, should always be no larger than 1 according to the Pauli principle. The one body occupation number reads

$$\bar{f}_i = \sum_j \delta_{\tau_i \tau_j} \delta_{s_i s_j} \int_{h^3} f_j(\mathbf{r}, \mathbf{p}, t) d^3r d^3p, \quad (7)$$

where  $s_i$  and  $\tau_i$  are the third components of the spin and isospin of particle  $i$ . This method can efficiently prevent the phase space distribution from evolving into a classical distribution from the initial nuclear ground state distribution.

In this model, the effective interaction potential energy can be written as

$$U = U_{\text{vol}} + U_{\text{sym}} + U_{\text{surf}} + U_{\text{eff}} + U_{\text{coul}}, \quad (8)$$

where the volume term, symmetry term, surface term, effective mass term and Coulomb term are expressed respectively by

$$U_{\text{vol}} = \frac{\alpha}{2} \sum_i \sum_{j \neq i} \frac{\rho_{ij}}{\rho_0} + \frac{\beta}{1+\gamma} \sum_i \left(\sum_{i \neq j} \rho_{ij} / \rho_0\right)^\gamma, \quad (9)$$

$$U_{\text{sym}} = \frac{C_{\text{sym}}}{2} \sum_i \sum_{j \neq i} t_{iz} t_{jz} \frac{\rho_{ij}}{\rho_0} \left(1 - k_{\text{sym}} \left[\frac{3}{2L} - \left(\frac{\mathbf{r}_i - \mathbf{r}_j}{2L}\right)^2\right]\right), \quad (10)$$

$$U_{\text{surf}} = \frac{g_{\text{surf}}}{2} \sum_i \sum_{j \neq i} \left[\frac{3}{2L} - \left(\frac{\mathbf{r}_i - \mathbf{r}_j}{2L}\right)^2\right] \frac{\rho_{ij}}{\rho_0}, \quad (11)$$

$$U_{\text{eff}} = g_\tau \sum_i \left(\sum_{i \neq j} \rho_{ij} / \rho_0\right)^\eta, \quad (12)$$

$$\begin{aligned} U_{\text{coul}} &= \frac{e^2}{4} \sum_i \sum_{j \neq i} \frac{1}{r_{ij}} (1+t_{iz})(1+t_{jz}) \\ &\quad \times \text{erf}(r_{ij}/\sqrt{4L}), \end{aligned} \quad (13)$$

where

$$\rho_{ij} = \frac{1}{(4\pi L)^{3/2}} \exp\left[-\frac{(\mathbf{r}_i - \mathbf{r}_j)^2}{4L}\right]. \quad (14)$$

The parameters used in this work are  $\alpha = -356.0$  MeV,  $\beta = 303.0$  MeV,  $\gamma = 7/6$ ,  $C_{\text{sym}} = 32.0$  MeV,  $k_{\text{sym}} = 0.08$  fm<sup>2</sup>,  $g_{\text{surf}} = 8.0$  MeV fm<sup>2</sup>,  $g_{\tau} = 10.0$  MeV,  $\eta = 2/3$  and  $\rho_0 = 0.165$  fm<sup>-3</sup>.

The switch function is introduced into the surface term of the system [20], which connects the surface energies of the projectile and the target with that of the compound nucleus. Then the surface energy can be expressed as

$$U_{\text{sys}}^{\text{surf}} = (U_{\text{poj}}^{\text{surf}} + U_{\text{targ}}^{\text{surf}})S + U_{\text{comp}}^{\text{surf}}(1 - S), \quad (15)$$

where  $S$  is called the switch function, which is written as

$$\begin{aligned} S = & C_0 + C_1 \frac{R - R_{\text{low}}}{R_{\text{up}} - R_{\text{low}}} + C_2 \left( \frac{R - R_{\text{low}}}{R_{\text{up}} - R_{\text{low}}} \right)^2 \\ & + C_3 \left( \frac{R - R_{\text{low}}}{R_{\text{up}} - R_{\text{low}}} \right)^3 + C_4 \left( \frac{R - R_{\text{low}}}{R_{\text{up}} - R_{\text{low}}} \right)^4 \\ & + C_5 \left( \frac{R - R_{\text{low}}}{R_{\text{up}} - R_{\text{low}}} \right)^5, \end{aligned} \quad (16)$$

where  $R$  is the distance of the centers between the projectile and the target, and  $R_{\text{up}}$  and  $R_{\text{low}}$  are the distance between the centers at the initial time and the final time when the compound nucleus is formed, respectively. The parameters  $C_0$ ,  $C_1$ ,  $C_2$ ,  $C_3$ ,  $C_4$  and  $C_5$  are 0, 0, 0, 10, -15 and 6, respectively, which make the continuity of the surface energy and its first derivative.

The importance of shell correction on the production cross section of compound nuclei has received much attention for the synthesis of superheavy elements [21, 22]. Consequently, it is necessary that the shell effect is considered in the fusion process. The projectile-target levels in the fusion reaction are calculated by the deformed two-center shell model (DTCSM) [22]. Then the shell corrections are calculated using the Strutinsky method [23]. In the ImIQMD model, the shell correction energy can be written as

$$U_{\text{shell}}^{\text{ImIQMD}} = - \int \frac{E_{\text{shell}} \exp[(r - R^{p(t)})/a]}{a \{1 + \exp[(r - R^{p(t)})/a]\}^2} dr. \quad (17)$$

Here,  $R^{p(t)}$  and  $a$  are the projectile(target) radius and the dispersion width, respectively. The values of  $R^{p(t)}$  and  $a$  are  $1.2 A^{-1/3}$  fm and 0.55 fm. In the evolution of the dynamical process, the ordering of filling in the levels is considered according to the angular momentum and the single nucleon energy, which correspond to the same angular momentum.

### 3 Results and discussions

As shown in Figs. 1–4, the shell corrections are displayed for the reaction systems  $^{12}\text{C}+^{14}\text{N}$ ,  $^{10}\text{B}+^{16}\text{O}$ ,  $^{17}\text{O}+^{13}\text{C}$ ,  $^{18}\text{O}+^{12}\text{C}$ ,  $^{19}\text{F}+^{19}\text{F}$ ,  $^{11}\text{B}+^{27}\text{Al}$ ,  $^{32}\text{S}+^{138}\text{Ba}$  and  $^{28}\text{Si}+^{142}\text{Ce}$  that lead to the same compound nuclei  $^{26}\text{Al}$ ,  $^{30}\text{Si}$ ,  $^{38}\text{Ar}$  and  $^{170}\text{Hf}$ .  $R_n = (R - R_f)/(R_t - R_f)$  is the normalized distance between centers, where  $R$  is the distance between centers,  $R_f = a_0 - a_2$  is the final  $R$ ,  $R_t = a_1 + a_2$  is the touching point distance, and  $a_0$ ,  $a_1$ , and  $a_2$  are the compound nucleus, target and projectile nucleus radius, respectively. From Fig. 1 it can be seen that at  $R_n > 0.2$  reaction  $^{10}\text{B}+^{16}\text{O}$  takes the lower shell correction  $E_{\text{shell}}$  values. This behavior probably results from the double magicity of  $^{16}\text{O}$ . However, at  $R_n < 0.2$ , the shell correction values show similar behaviors in two reactions. In Fig. 2, one can see that  $^{17}\text{O}+^{13}\text{C}$  takes the lower shell correction values at  $R_n > 0.3$  but the values are almost the same as the reaction  $^{18}\text{O}+^{12}\text{C}$  at  $R_n < 0.3$ . This is a possible consequence that  $^{17}\text{O}$  has a magic proton number  $Z=8$  and  $8+1$  neutrons, being the closest to the double magicity. It can be seen that  $^{19}\text{F}+^{19}\text{F}$  takes the lower shell correction values at  $R_n > 0.8$  in Fig. 3, which may result from the fact that  $^{19}\text{F}$  is close to the magic proton number  $Z=8$ . Due to the magic neutron number of  $^{138}\text{Ba}$  in Fig. 4, one can see that  $^{32}\text{S}+^{138}\text{Ba}$  takes the lower shell correction values at  $R_n > 1.09$ . From the above discussions, one can see that the trends of shell correction are similar for  $^{12}\text{C} + ^{14}\text{N}$  and  $^{10}\text{B}+^{16}\text{O}$ ,  $^{17}\text{O}+^{13}\text{C}$  and  $^{18}\text{O}+^{12}\text{C}$ ,  $^{32}\text{S}+^{138}\text{Ba}$  and  $^{28}\text{Si}+^{142}\text{Ce}$  due to the small difference in mass asymmetry. However, for the symmetric combination  $^{19}\text{F}+^{19}\text{F}$  and asymmetric combination  $^{11}\text{B}+^{27}\text{Al}$ , the trends of curves are different. This indicates that the mass asymmetry might play an important role in fusion reactions.

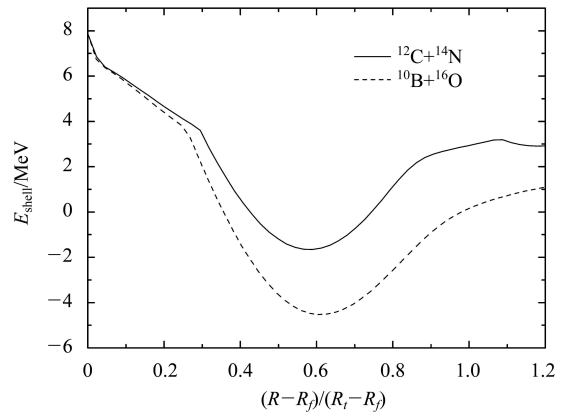


Fig. 1. Shell corrections for two fusion reactions in the synthesis of  $^{26}\text{Al}$ .

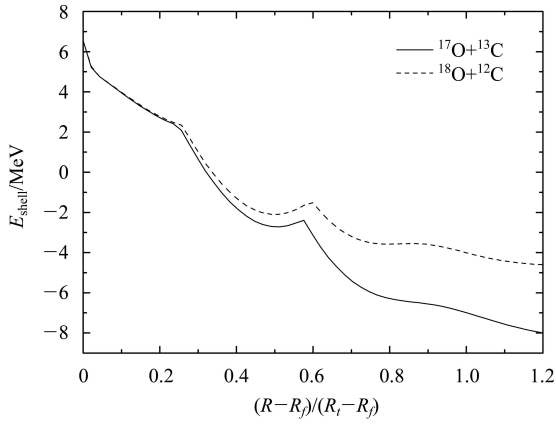


Fig. 2. Shell corrections for two fusion reactions in the synthesis of  $^{30}\text{Si}$ .

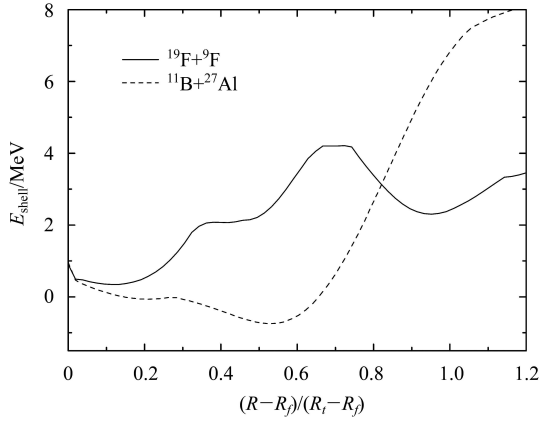


Fig. 3. Shell corrections for two fusion reactions in the synthesis of  $^{38}\text{Ar}$ .

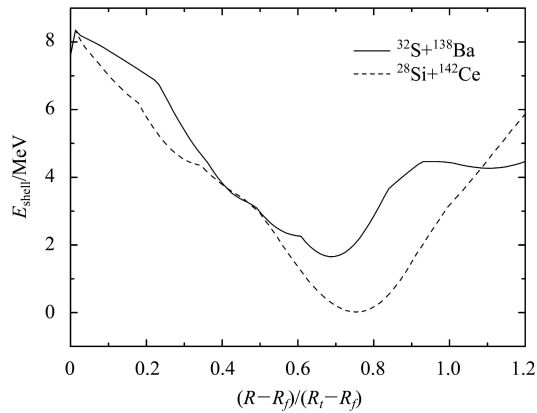


Fig. 4. Shell corrections for two fusion reactions in the synthesis of  $^{170}\text{Hf}$ .

The nucleus-nucleus interaction potential plays an important role in the fusion reaction. Many methods, such as Wong's semiempirical formula [24], the Bass potential [25], the proximity potential [26] and the

adiabatic potential [27], have been used to calculate the Coulomb barrier. In this work, the effects of the mass asymmetry of the projectile and the target on the static Coulomb barrier are studied by calculating the static Coulomb barrier. The interaction potential is defined as  $V(R) = E_{pt}(R) - E_p - E_t$ . Here,  $R$  is the distance between the centers of mass of the projectile and the target.  $E_{pt}(R)$  is the total energy of the whole system, while  $E_p$  and  $E_t$  are the energies of the projectile and the target, respectively. They are the sum of the effective potential energy and the kinetic energy over the whole system, projectile and target, respectively. For kinetic energy, the Thomas-Fermi approximation is adopted, as mentioned in Ref. [28]. For the static Coulomb barrier, the density distribution is the same as the initial density distribution, which is the adiabatic process. In Table 1, we compare the static Coulomb barriers calculated by the ImIQMD model with the results of the Bass potential and the proximity potential. The effects of the mass asymmetry of the projectile and the target on the Coulomb barriers are observed in all reactions. One can see that the symmetric combinations will give rise to higher Coulomb barriers, and with increasing mass asymmetry, the height of the Coulomb barrier decreases and the capture probability should be enhanced consequently [28]. Thus it is more favorable to form the superheavy elements using more asymmetric reaction systems. We will investigate the effect of mass asymmetry by calculating the fusion cross sections later.

Table 1. Comparison of the static Coulomb barriers calculated by the ImIQMD model with the results of the Bass potential and the proximity potential. (Unit:MeV)

reaction	$V_b^{\text{ImIQMD}}$	$V_b^{\text{Prox.}}$	$V_b^{\text{Bass}}$
$^{12}\text{C}+^{14}\text{N}$	6.29	7.56	7.49
$^{10}\text{B}+^{16}\text{O}$	6.06	7.23	7.16
$^{17}\text{O}+^{13}\text{C}$	7.04	8.45	8.22
$^{18}\text{O}+^{12}\text{C}$	7.34	8.37	8.19
$^{19}\text{F}+^{19}\text{F}$	12.17	13.61	13.33
$^{11}\text{B}+^{27}\text{Al}$	9.13	10.95	10.83
$^{32}\text{S}+^{138}\text{Ba}$	100.11	110.15	110.57
$^{28}\text{Si}+^{142}\text{Ce}$	95.32	100.61	100.88

Figures 5–8 present the calculated fusion cross sections compared with the experimental data [29–32] for  $^{12}\text{C}+^{14}\text{N}$ ,  $^{10}\text{B}+^{16}\text{O}$ ,  $^{17}\text{O}+^{13}\text{C}$ ,  $^{18}\text{O}+^{12}\text{C}$ ,  $^{19}\text{F}+^{19}\text{F}$ ,  $^{11}\text{B}+^{27}\text{Al}$ ,  $^{32}\text{S}+^{138}\text{Ba}$  and  $^{28}\text{Si}+^{142}\text{Ce}$ . It can be seen that our model calculations agree with the experimen-

tal data for  $^{12}\text{C}+^{14}\text{N}$ ,  $^{10}\text{B}+^{16}\text{O}$ ,  $^{19}\text{F}+^{19}\text{F}$  and  $^{11}\text{B}+^{27}\text{Al}$ . In Fig. 6 and Fig. 8, the calculated results are larger than the experimental data. One notes that this result is more obvious for  $^{17}\text{O}+^{13}\text{C}$  than that for  $^{18}\text{O}+^{12}\text{C}$ . This phenomenon probably results from the consequence that  $^{17}\text{O}$  has magic proton number  $Z=8$  and  $8+1$  neutrons, being the closest to the double magicity which may play an important role in the fusion reaction in terms of the analysis of the above shell corrections. For a clear departure from data in Fig. 6 and Fig. 8, a possible way of explaining it is without considering the zero-point motion of the nuclear surface related to low-lying collective vibrations. Although a departure from data occurs, one can find that there is an enhancement of the cross sections for the reactions  $^{12}\text{C}+^{14}\text{N}$ ,  $^{10}\text{B}+^{16}\text{O}$ ,  $^{17}\text{O}+^{13}\text{C}$ ,  $^{18}\text{O}+^{12}\text{C}$ ,  $^{32}\text{S}+^{138}\text{Ba}$  and  $^{28}\text{Si}+^{142}\text{Ce}$ , which results

from the lowering of the Coulomb barrier for the reactions with larger mass asymmetry. But for the asymmetric reaction  $^{19}\text{F}+^{19}\text{F}$  and asymmetric reaction  $^{11}\text{B}+^{27}\text{Al}$ , the enhancement of the fusion cross sections is not obvious at lower energies. An abrupt increase at the higher energies is shown for the symmetric system  $^{19}\text{F}+^{19}\text{F}$ , which is in contradiction with the previous results [16]. Maybe the experimental data that include complete and incomplete fusion processes without distinction result in this discrepancy. In Ref. [31], the fusion barriers and values for the fusion inhibition factor extracted from the data indicate that an asymmetric system favors fusion. The present results suggest that the fusion of a system with larger mass asymmetry is favorable for the formation of compound nuclei because of the smaller Coulomb contribution to the fusion barrier.

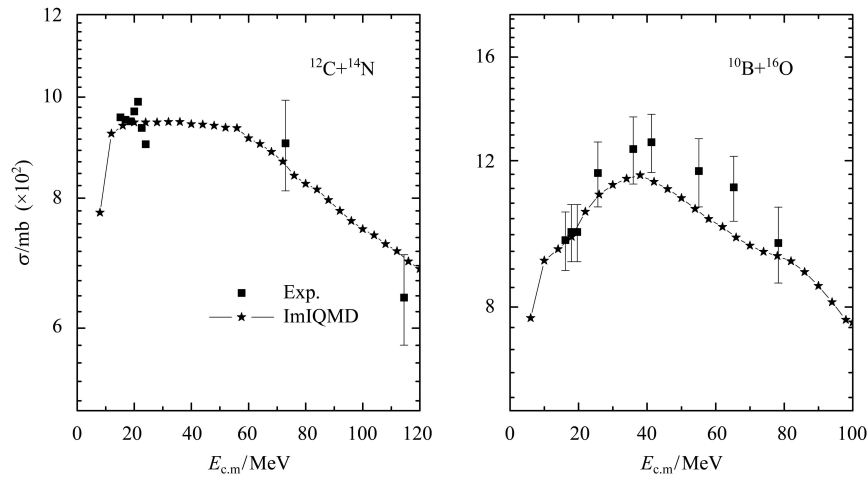


Fig. 5. Comparison of the calculated fusion cross section with the experimental data for  $^{12}\text{C}+^{14}\text{N}$  and  $^{10}\text{B}+^{16}\text{O}$  systems. Solid squares represent the experimental data and the crosses represent the calculated results.

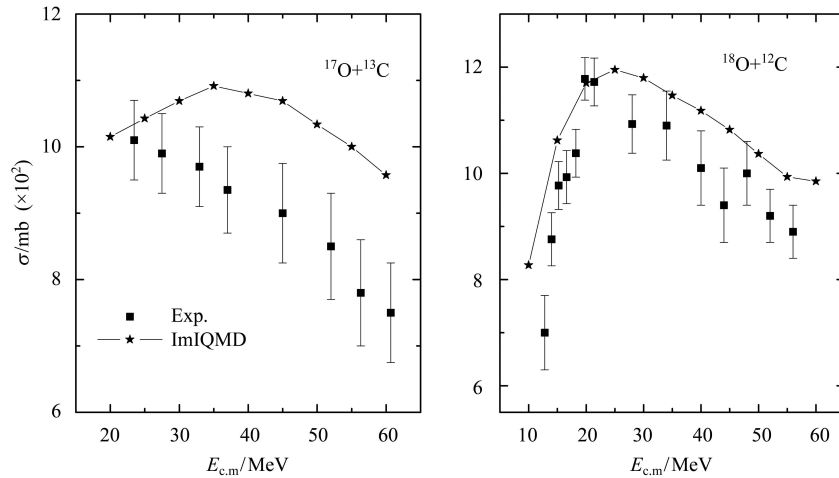


Fig. 6. The same as in Fig. 5, but for systems  $^{17}\text{O}+^{13}\text{C}$ ,  $^{18}\text{O}+^{12}\text{C}$ .

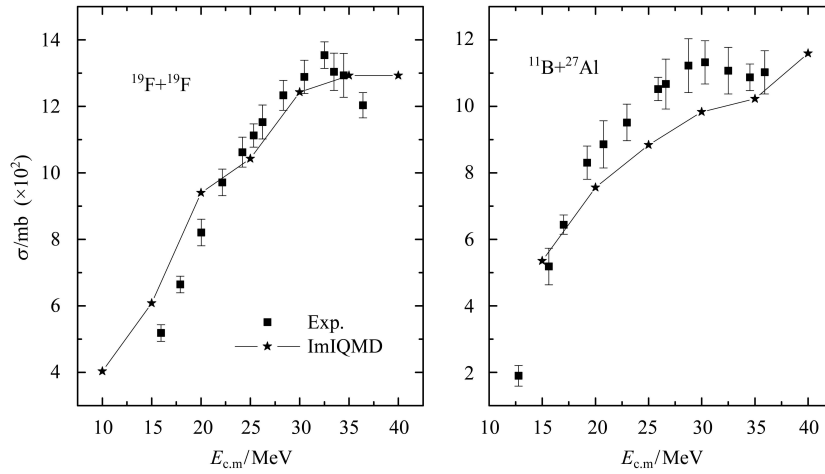


Fig. 7. The same as in Fig. 5, but for systems  $^{19}\text{F}+^{19}\text{F}$ ,  $^{11}\text{B}+^{27}\text{Al}$ .

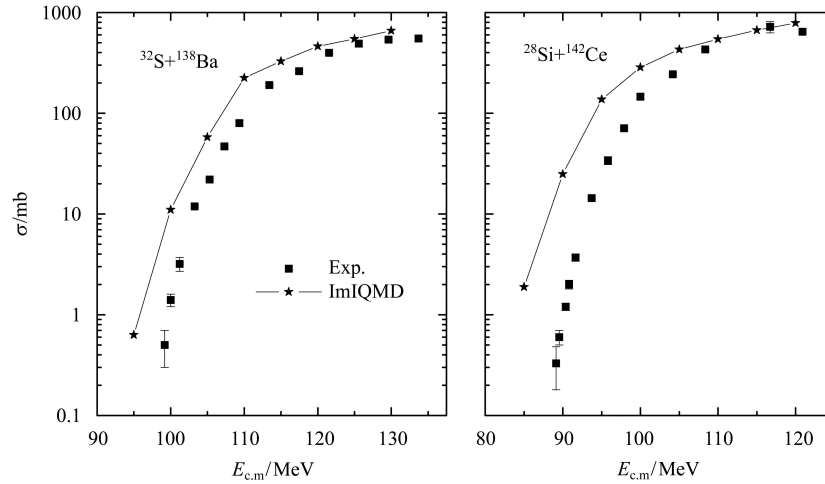


Fig. 8. The same as in Fig. 5, but for systems  $^{32}\text{S}+^{138}\text{Ba}$  and  $^{28}\text{Si}+^{142}\text{Ce}$ .

## 4 Conclusion

In conclusion, we have investigated the symmetric and asymmetric reaction systems forming the same compound nuclei  $^{26}\text{Al}$ ,  $^{30}\text{Si}$ ,  $^{38}\text{Ar}$  and  $^{170}\text{Hf}$  using the ImIQMD model. The Coulomb barrier is lower with large mass asymmetry than that with small mass asymmetry. The experimental data of the fusion cross sections have been reproduced quantitatively. The

results show that the fusion cross sections are larger for the reaction system with larger mass asymmetry, which results from the lowering of the Coulomb barrier for the system with larger mass asymmetry. Thus the compound nucleus formation is more favorable for the system with the larger mass asymmetry. This indicates that the choice of the systems leading to the same compound nucleus with different mass asymmetry is sensitive to seek the difference between the fusion cross sections.

## References

- 1 Ćwiok S, Dobaczewski J, Heenen P H et al. Nucl. Phys. A, 1996, **611**: 211–246
- 2 Rutz K, Bender M, Bürvenich T et al. Phys. Rev. C, 1997, **56**: 238–243
- 3 Bender M, Rutz K, Reinhard P G et al. Phys. Rev. C, 1999, **60**: 034304
- 4 Kruppa A T, Bender M, Nazarewicz W et al. Phys. Rev. C, 2000, **61**: 034313
- 5 Bender M, Nazarewicz W, Reinhard P G. Phys. Lett. B, 2001, **515**: 42–48
- 6 Hofmann S, Münzenberg G. Rev. Mod. Phys., 2000, **72**: 733
- 7 Hofmann S, Heßberger F P, Ackermann D et al. Eur. Phys. J. A, 2001, **10**: 5–10
- 8 Oganessian Yu Ts, Utyonkoy V K, Lobanov Yu V et al. Phys. Rev. C, 2004, **69**:021601(R)

- 9 Adamian G G, Antonenko N V, Scheid W et al. Nucl. Phys. A, 1997, **627**: 361–378
- 10 Aritomo Y, Wada T, Ohta M et al. Phys. Rev. C, 1999, **59**: 796–809
- 11 Zagrebaev V I. Phys. Rev. C, 2001, **64**: 034606
- 12 Govil I M, Singh R, Kumar A et al. Nucl. Phys. A, 2000, **674**: 377–393
- 13 Prasad N V S V, Vinodkumar A M, Sinha A K et al. Nucl. Phys. A, 1996, **603**: 176–202
- 14 Fazio G, Giardina G, Mandaglio G et al. Phys. Rev. C, 2005, **72**: 064614
- 15 FENG Zhao-Qing, ZHANG Feng-Shou, JIN Gen-Ming et al. Nucl. Phys. A, 2005, **750**: 232–244
- 16 BIAN Bao-An, ZHANG Feng-Shou, ZHOU Hong-Yu. Phys. Lett. B, 2008, **665**: 314–317
- 17 BIAN Bao-An, ZHANG Feng-Shou, ZHOU Hong-Yu. Nucl. Phys. A, 2009, **829**: 1–12
- 18 WANG Ning, WU Xi-Zhen, LI Zhu-Xia. Phys. Rev. C, 2003, **67**: 024604
- 19 Papa M, Maruyama T, Bonasera A. Phys. Rev. C, 2001, **64**: 024612
- 20 FENG Zhao-Qing, JIN Gen-Ming, ZHANG Feng-Shou et al. High Energy Phys. and Nucl. Phys., 2005, **29**(12): 1157–1161 (in Chinese)
- 21 Gherghescu R A, Skalski J, Patyk Z et al. Nucl. Phys. A, 1999, **651**: 237–249
- 22 Gherghescu R A, Greiner W, Münzenberg G. Phys. Rev. C, 2003, **68**: 054314
- 23 Strutinsky V M. Nucl. Phys. A, 1967, **95**: 420–442
- 24 WONG C Y. Phys. Rev. Lett., 1973, **31**: 766–799
- 25 Bass R. Nuclear Reactions with Heavy Ions. New York, Springer, 1980. 283
- 26 Myers W D, Swiatecki W J. Phys. Rev. C, 2000, **62**: 044610
- 27 Siwek-Wilczyńska K, Wilczyński J. Phys. Rev. C, 2001, **64**: 024611
- 28 Denisov V Yu, Norenberg W. Eur. Phys. J. A, 2002, **15**: 375–388
- 29 Vandenbosch R, Lazzarini A J. Phys. Rev. C, 1981, **23**: 1074–1079
- 30 Heusch B, Beck C, Coffin J P et al. Phys. Rev. C, 1982, **26**: 542–554
- 31 Anjos R M, Guiarães V, Added N et al. Phys. Rev. C, 1990, **42**: 354–362
- 32 Gil S, Hasenbalg F, Testoni J E et al. Phys. Rev. C, 1995, **51**: 1336–1344